

Machine learning for uncertainty estimation in fusing precipitation observations from satellites and ground-based gauges

Georgia Papacharalampous^{1,*}, Hristos Tyralis², Nikolaos Doulamis³, Anastasios Doulamis⁴

¹ Department of Topography, School of Rural, Surveying and Geoinformatics Engineering, National Technical University of Athens, Iroon Polytechniou 5, 157 80 Zografou, Greece (papacharalampous.georgia@gmail.com, gpapacharalampous@hydro.ntua.gr, <https://orcid.org/0000-0001-5446-954X>)

² Department of Topography, School of Rural, Surveying and Geoinformatics Engineering, National Technical University of Athens, Iroon Polytechniou 5, 157 80 Zografou, Greece (montchrister@gmail.com, hristos@itia.ntua.gr, <https://orcid.org/0000-0002-8932-4997>)

³ Department of Topography, School of Rural, Surveying and Geoinformatics Engineering, National Technical University of Athens, Iroon Polytechniou 5, 157 80 Zografou, Greece (ndoulam@cs.ntua.gr, <https://orcid.org/0000-0002-4064-8990>)

⁴ Department of Topography, School of Rural, Surveying and Geoinformatics Engineering, National Technical University of Athens, Iroon Polytechniou 5, 157 80 Zografou, Greece (adoulam@cs.ntua.gr, <https://orcid.org/0000-0002-0612-5889>)

* Corresponding author

Abstract: To form precipitation datasets that are accurate and, at the same time, have high spatial densities, data from satellites and gauges are often merged in the literature. However, uncertainty estimates for the data acquired in this manner are scarcely provided, although the importance of uncertainty quantification in predictive modelling is widely recognized. Furthermore, the benefits that machine learning can bring to the task of providing such estimates have not been broadly realized and properly explored through benchmark experiments. The present study aims at filling in this specific gap by conducting the first benchmark tests on the topic. On a large dataset that comprises 15-year-long monthly data spanning across the contiguous United States, we extensively compared six learners that are, by their construction, appropriate for predictive uncertainty quantification. These are the quantile regression (QR), quantile regression forests (QRF), generalized random forests (GRF), gradient boosting machines (GBM), light gradient boosting machines (LightGBM) and quantile regression neural networks

(QRNN). The comparison referred to the competence of the learners in issuing predictive quantiles at nine levels that facilitate a good approximation of the entire predictive probability distribution, and was primarily based on the quantile and continuous ranked probability skill scores. Three types of predictor variables (i.e., satellite precipitation variables, distances between a point of interest and satellite grid points, and elevation at a point of interest) were used in the comparison and were additionally compared with each other. This additional comparison was based on the explainable machine learning concept of feature importance. The results suggest that the order from the best to the worst of the learners for the task investigated is the following: LightGBM, QRF, GRF, GBM, QRNN and QR. The respective order of the three types of predictors considered in the experiments is the following: Satellite precipitation, elevation and distances.

Keywords: bias correction; light gradient boosting machine; probabilistic prediction; quantile regression; spatial interpolation; uncertainty quantification

1. Introduction

Satellite and gauge-measured precipitation data are often merged under the important scope of forming datasets that are accurate and, at the same time, have high spatial densities (Hu et al. 2019, Abdollahipour et al. 2022). This is indeed necessary, as economic constraints often prohibit investments in highly spatially dense gauge networks, and is commonly referred to as “satellite precipitation product correction”. Notably, even data that have already been obtained through the fusion of satellite and gauge-measured data can become more accurate by taking further advantage of gauge-measured data (Tyrallis et al. 2023a). Consequently, for the sake of simplicity, such mixed-type data will not be distinguished hereinafter from pure satellite observations (and mixed-type data and datasets will be sometimes referred to as “satellite” data and datasets), given also that the technicalities of their fusion with pure gauge-based observations are exactly the same.

A well-known fact is that most of the studies devoted to satellite precipitation product correction provide the mean of the predictive probability distribution. Among others, this can be achieved by using standard regression algorithms (e.g., those described in Hastie et al. 2009, James et al. 2013, Efron and Hastie 2016) for spatial interpolation. Relevant works were conducted, for example, by Baez-Villanueva et al. (2020), Chen et al. (2020), Nguyen et al. (2021), Fernandez-Palomino et al. (2022) and Papacharalampous et al. (2023a).

However, entire predictive probability distributions or adequate approximations of them should be preferred when possible (Gneiting and Raftery 2007) due to the larger amount of information that they offer, thereby allowing better decision making than the prediction of the mean alone. Such predictive uncertainty estimates (i.e., probabilistic predictions) appear more and more frequently in other fields (e.g., in Rodrigues and Pereira 2020, Kasraei et al. 2021, Cui et al. 2022) and in other hydrological disciplines (e.g., in Weerts et al. 2011, Tareghian and Rasmussen 2013, Papacharalampous et al. 2020, Tyralis and Papacharalampous 2021b, Tyralis et al. 2023b), but have only been provided by a few studies in the field of satellite precipitation product correction with machine learning (Bhuiyan et al. 2018, Zhang et al. 2022, Glawion et al. 2023 and Tyralis et al. 2023a). Still, each of these studies uses a single algorithm and the one by Tyralis et al. (2023a) additionally focuses on extreme events. Therefore, the benefits that machine learning can bring to the general task of predictive uncertainty quantification in merging satellite and gauge-measured precipitation data have not been sufficiently explored so far.

The aim of this work was to fill in this specific gap for advancing the state of the machine learning-driven applications of predictive uncertainty quantification in merging precipitation observations from satellites and ground-based gauges. This was achieved though extensively investigating the machine learning concept of quantile regression for fulfilling this task. Indeed, as the various quantile regression algorithms exhibit different relative performances at different prediction problems (see diverging results from other fields, for example, in Zhang et al. 2018, He et al. 2019, Sesia and Candès 2020), a comparison between alternative implementations in the field of the concept of interest was necessary.

This comparison had to be of large scale according to the guidelines by Boulesteix et al. (2018) to ensure that its output is as general as possible for the problem of interest. This translates to using data that cover a large spatial region and a large time period, and to including several learners and a large number of predictors in the experiments. Notably, such large-scale comparisons are rare in the literature that merges data from satellites and ground-based gauges (Papacharalampous et al. 2023a).

The remaining article is arranged as follows: Section 2 provides important information about the learners that were extensively compared by this work for the general task of estimating predictive uncertainty in blending precipitation observations from satellites and ground-based gauges. Section 3 presents the dataset and procedures used for the

comparison. [Section 4](#) presents the large-scale results. [Section 5](#) discusses several outputs of the comparison under the spectrum that the current literature provides and proposes ideas for future investigations. [Section 6](#) presents the concluding remarks. To ensure the reproducibility of the methods and tests of this work, [Appendix A](#) is devoted to statistical software information. This latter information could be used alongside with the parameter settings described in [Section 2](#).

2. Learners for uncertainty estimation

2.1 Quantile regression

Quantile regression (QR; Koenker and Bassett [1978](#), Koenker [2005](#)) is the simplest learner used in this work for estimating predictive uncertainty in blending precipitation data from satellites and ground-based gauges, and is trained by minimizing across the various samples the quantile scoring function (Gneiting [2011](#)). The latter is defined in [Section 3.4](#). Tutorial information about QR can be found in Waldmann ([2018](#)).

2.2 Quantile regression forests

Quantile regression forests (QRF; Meinshausen and Ridgeway [2006](#)) are a variant of random forests (Breiman [2001](#)) for predictive uncertainty quantification. Random forests fall into the category of ensemble learning algorithms (Sagi and Rokach [2018](#)). They grow an ensemble of decision trees (Breiman et al. [1984](#)) by running bootstrap aggregation (bagging; Breiman [1996](#)) coupled with an additional randomization procedure. While, in standard regression, the output prediction is the mean of the predictions of all the decision trees (with this mean approximating the conditional mean of the response variable), for QRF it is a resemblance of the conditional distribution of the response variable. In this work, QRF were implemented with 500 decision trees. The other parameters of QRF were set to their defaults in Tibshirani and Athey ([2023](#)).

2.3 Generalized random forests

Generalized random forests (GRF; Athey et al. [2019](#)) are another variant of random forests for uncertainty quantification that are expected to model heterogeneities better than QRF. In this work, GRF were implemented with 500 decision trees. The other parameters of GRF were set to their defaults in Tibshirani and Athey ([2023](#)).

2.4 Gradient boosting machines

Gradient boosting machines (GBM; Friedman 2001) are a boosting (Mayr et al. 2014, Tyralis and Papacharalampous 2021a) variant that can be used, among others, for predictive uncertainty quantification. A boosting algorithm is an ensemble learning algorithm that composes a strong learner by sequentially adding weak base learners to the ensemble. Specifically, the training of every new base learner targets at minimizing the error of the current ensemble. This error is the quantile loss (Gneiting 2011) for the case of GBM. Notably, the number of times that a new base learner is added to the ensemble (which is the same with the number of base learners) should be that large that it ensures proper fitting simultaneously avoiding overfitting. In this work, GBM employed 500 decision trees as their base learners. The other parameters of GBM were set to their defaults in Greenwell et al. (2022).

2.5 Light gradient boosting machines

Light gradient boosting machines (LightGBM; Ke et al. 2017) are the second boosting variant used in this work. They are known to have some better properties (e.g., smaller training time) compared to GBM (Tyralis and Papacharalampous 2021a). In this work, they were implemented with decision trees as base learners. The maximum tree depth, the maximum number of leaves in one tree, the minimal number of data in one leaf, the shrinkage rate, the number of boosting iterations (number of trees), the feature fraction that is randomly selected on each iteration (tree), the data fraction that is randomly selected without resampling on each iteration (tree), the minimal gain to perform split and the number of threads were equal to 10, 500, 200, 0.05, 400, 0.75, 0.75, 0 and 10, respectively. These are parameter values that were previously identified as optimal in Tyralis et al. (2023a). The other parameters of LightGBM were set to their defaults in Shi et al. (2023).

2.6 Quantile regression neural networks

Quantile regression neural networks (QRNN; Taylor 2000, Cannon 2011) are a neural network (Hastie et al. 2009, chapter 11) algorithm that can, by its construction, facilitate uncertainty quantification. In modelling with neural networks, linear combinations of the predictors are first defined. Then, the form of a non-linear function of these combinations is given to the dependent variable. In this work, QRNN were run with a number of

repeated trials equal to 1. The other parameters of QRNN were set to their defaults in Cannon (2023).

3. Data, application and comparison

3.1 Data

To evaluate and compare the learners, three types of data were used. These are gauge-measured precipitation (see Section 3.1.1), satellite precipitation (see Section 3.1.2) and elevation (see Section 3.1.3) data. Note that the same data compilation was previously used for different benchmarking purposes in Papacharalampous et al. (2023c).

3.1.1 Gauge-measured precipitation data

Monthly precipitation totals from ground-based gauges were extracted from the Global Historical Climatology Network monthly database, version 2 (GHCNm) (Peterson and Vose 1997). The extraction took place through the repository of the National Oceanic and Atmospheric Administration (NOAA), which is available online in the following address (accessed on 2022-09-24): <https://www.ncei.noaa.gov/pub/data/ghcn/v2>. The gauge-measured data refer to 1 421 locations (see Figure 1) in the contiguous United States (CONUS) and to the time period starting from 2001 and ending with 2015.

3.1.2 Satellite precipitation data

Precipitation data from satellites were extracted from two databases, specifically the current operational PERSIANN (Precipitation Estimation from Remotely Sensed Information using Artificial Neural Networks) database (Hsu et al. 1997, Nguyen et al. 2018, 2019) and the GPM IMERG (Integrated Multi-satellitE Retrievals) late Precipitation L3 1 day 0.1 degree x 0.1 degree V06 database (Huffman et al. 2019). These databases were formed by the Centre for Hydrometeorology and Remote Sensing (CHRS) of the University of California, Irvine (UCI) and the NASA (National Aeronautics and Space Administration) Goddard Earth Sciences (GES) Data and Information Services Center (DISC), respectively.

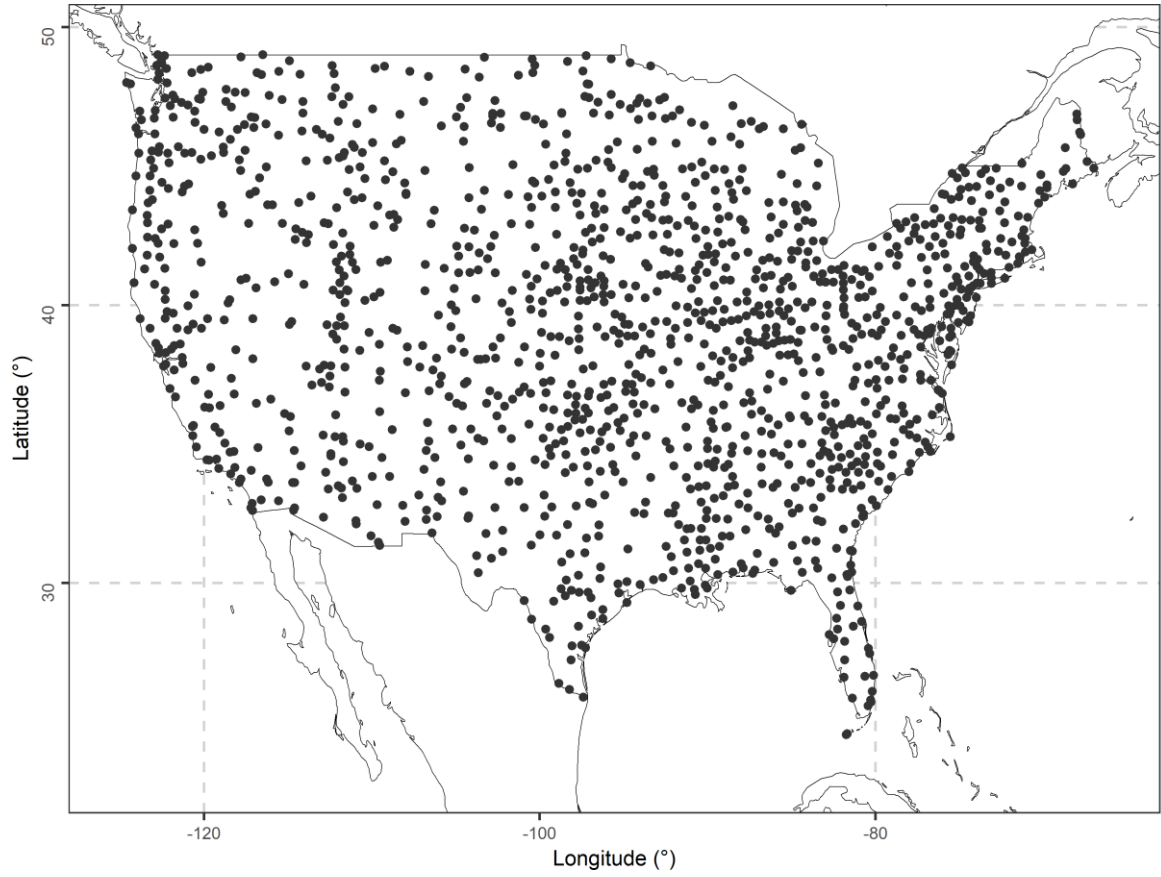


Figure 1. Locations of the ground-based gauges that recorded data used in this study.

In particular, the extraction of gridded satellite data was conducted from the CHRS and the NASA Earth Data repositories, which are available online in the following addresses (accessed on 2022-03-07 and 2022-12-10, respectively): <https://chrsdata.eng.uci.edu> and <https://doi.org/10.5067/GPM/IMERGDL/DAY/06>. The satellite data extracted were daily precipitation data and referred to the time period starting from 2001 and ending with 2015. The PERSIANN and IMERG grids extracted cover the CONUS entirely and have a spatial resolution of 0.25 degree x 0.25 degree and 0.1 degree x 0.1 degree, respectively. Bilinear interpolation was applied to the IMERG grid extracted to transform it to the CMORPH0.25 grid with a spatial resolution of 0.25 degree x 0.25 degree. The latter IMERG grid was used in the experiments of this work, together with the PERSIANN grid extracted. Additionally, total monthly precipitation data was obtained by aggregating the daily data for conforming to requirements of the same experiments.

3.1.3 Elevation data

Because of its well-recognised usefulness as a predictor for many hydrometeorological variables (Xiong et al. 2022), elevation was estimated at the locations of the ground-based gauges (which are depicted in Figure 1). The estimation was based on the Amazon Web Services (AWS) Terrain Tiles. The latter are available online in the following address (accessed on 2022-09-25): <https://registry.opendata.aws/terrain-tiles>.

3.2 Spatial interpolation setting and validation method

Figure 2 illustrates how the spatial interpolation problem was formulated for facilitating the experiments of this work. The gauge-measured total monthly precipitation at a geographical location of interest is the dependent variable. Following procedures proposed in previous works (Papacharalampous et al. 2023a, b, c and Tyrallis et al. 2023a), the four closest grid points from each grid to each ground-based station (see Figure 1) were identified and indexed according to their distance from this station, which was computed in meters. The monthly precipitation totals at the four closest grid points 1–4 are hereinafter called “PERSIANN values 1–4” or “IMERG values 1–4”. Similarly, the distances d_i , $i = 1, 2, 3, 4$, where $d_1 < d_2 < d_3 < d_4$, are hereinafter called “PERSIANN distances 1–4” or “IMERG distances 1–4”. These total monthly precipitation values and distances are the predictor variables, together with the elevation at the station. The dataset includes 91 623 samples, which are used within a five-fold cross-validation setting.

3.3 Quantile levels and quantile crossing handling

A good approximation of the predictive probability distribution can be acquired by predicting quantiles of this distribution at multiple levels. In this study, the quantile levels $a \in \{0.025, 0.050, 0.100, 0.250, 0.500, 0.750, 0.900, 0.950, 0.975\}$ were investigated. Negative predictive quantiles at the lowest quantile level were censored to zero. Additionally, quantile crossing was handled by setting, separately for each pair {sample, learner}, any predictive quantile that was smaller than the predictive quantile of the immediate lower quantile level equal to this latter predictive quantile.

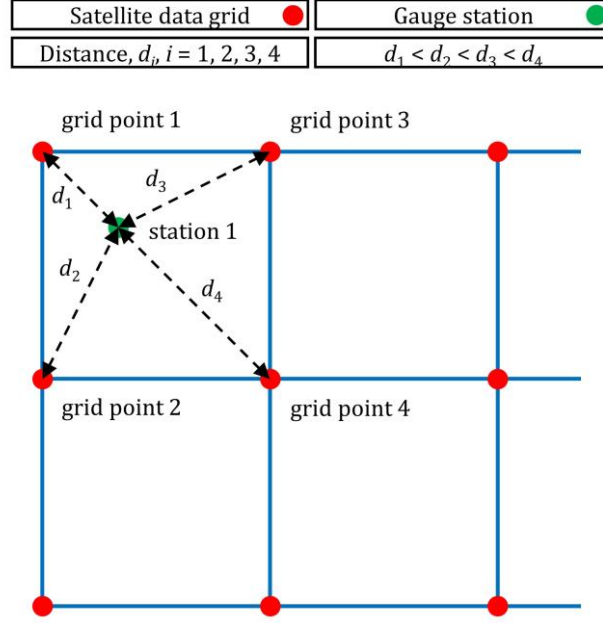


Figure 2. Illustration of how the spatial interpolation problem was formulated. The satellite precipitation data are available at grid points. The distances of a given station (station 1) from its four closest grid points (grid points 1–4) are denoted with $d_i, i = 1, 2, 3$ and 4. These distances and the monthly precipitation data from satellites at the same grid points were used as predictors for precipitation at the given station.

3.4 Performance comparison

To facilitate the comparison of the six learners (see [Section 2](#)) with respect to their performance at the nine quantile levels (see [Section 3.3](#)), the quantile scoring function was first computed. This function is defined as

$$L_a(z, y) := f_a(z - y), \quad (1)$$

where y is the realization of the precipitation process, z is the respective prediction (predictive quantile) at level a and $f_a(x)$ is defined as

$$f_a(x) := x (\mathbb{I}(x \geq 0) - a), \quad x \in \mathbb{R}, \quad (2)$$

where $\mathbb{I}(A)$ is the indicator function. This function is equal to 1 when the event A realizes. Otherwise, it is equal to 0.

Then, a performance criterion takes the form

$$\bar{L}_a(z, y) := (1/k) \sum_{i=1}^k L(z_i, y_i), \quad (3)$$

where x_i and $z_i, i \in \{1, \dots, k\}$ are, respectively, the prediction and observation of the i^{th} data sample and k is the number of data samples included in the test dataset. Obviously, this performance criterion was computed separately for each learning algorithm.

Quantile skill scores $L_{a,skill}$ were also computed for each learning algorithm and the entire dataset according to the equation

$$L_{a,skill} := 1 - \bar{L}_{a,learner} / \bar{L}_{a,benchmark}, \quad (4)$$

where the simplest algorithm (i.e., QR) is used as benchmark. The quantile skill score takes values between $-\infty$ and 1. The larger it is, the better the predictive quantiles of a learner on average compared to the predictive quantiles of the benchmark.

Quantile skill scores were additionally computed for each pair {learner, station} to examine how the relative performance of the learners varies from station to station for each quantile level.

Moreover, the quantile losses at the various quantile levels (computed as stated above using Equation (1)) were summed up for each pair {case, learner}. The sums acquired through this procedure were subsequently averaged across all the cases in the dataset, separately for each learner, thereby giving continuous ranked probability scores.

Then, following an equation similar to Equation (4), the latter scores were used to compute continuous ranked probability skill scores (Epstein 1969, Matheson and Winkler 1976, Gneiting and Raftery 2007). Indeed, the continuous ranked probability score of quantile predictions at multiple levels can be written as the sum of the respective quantile scores (Bröcker 2012), in the sense that quantile predictions can be viewed as ensemble members. Similar to the quantile skill score, the continuous ranked probability skill score takes values from $-\infty$ to 1 and the larger it is, the better the predictive performance with respect to the benchmark.

Continuous ranked probability skill scores were also computed for each pair {learner, station} to examine how the relative performance of the learners varies from station to station for the entire approximation of the predictive probability distribution.

Lastly, the reliability of the learners was examined by computing sample coverages. For this test, the frequency with which each predictive quantile is smaller or equal to its corresponding observation was first computed. The frequencies acquired through this procedure were then averaged, separately for each pair {learner, quantile level}. The closer a mean frequency to its nominal value, the more reliable the predictive quantiles.

3.5 Predictor variable importance comparison

Explainable machine learning can support, among others, predictor variable importance comparisons. For conducting such a comparison for the problem of interest in this study, LightGBM (see [Section 2.5](#)) were used. More precisely, the total gain in splits of each predictor variable (Shi et al. 2023) was computed through this learner for the entire dataset. Based on the respective results, the predictors were ranked from the most to the least important ones according to the following rule: The larger the total gain, the larger the importance.

4. Results

4.1 Performance comparison

[Figure 3](#) presents statistics that allow us to evaluate and compare the performance of the learners in the task of estimating predictive uncertainty while blending precipitation data from satellites and ground-based gauges. In terms of sample coverage (see [Figure 3a](#)), all the learners perform at least adequately well, with the best of them being QRF and GRF for quantile levels $\{0.025, 0.050, 0.100, 0.250\}$, QR and QRNN for the quantile level 0.500, and QR, GBM and QRNN for the remaining quantile levels.

While sample coverage offers some insight into the performance of the learners, an appropriate score to evaluate this performance at the quantile level is the quantile skill score. According to this (see [Figure 3b](#)), the best-performing learner is LightGBM. According to the same score, QRF, GRF, GBM, QRNN and QR are, respectively, ranked second, third, fourth, fifth and sixth for each of the quantile levels. The same ranking is obtained based on the continuous ranked probability skill score (see [Figure 3c](#)), which is appropriate for evaluating the quality of an ensemble of predictions at multiple quantile levels (with these predictions approximating an entire predictive probability distribution).

[Figure 4](#) allows us to assess to which degree the quantile skill score varies in space for the various learners and the various quantile levels, while [Figure 5](#) allows a similar assessment but for the continuous ranked probability skill score (which provides a proper assessment for the total of the quantile levels). Both scores are found to vary a lot from station to station. Also notably, good and bad performances with respect to the benchmark tend to appear at the same stations for multiple methods.

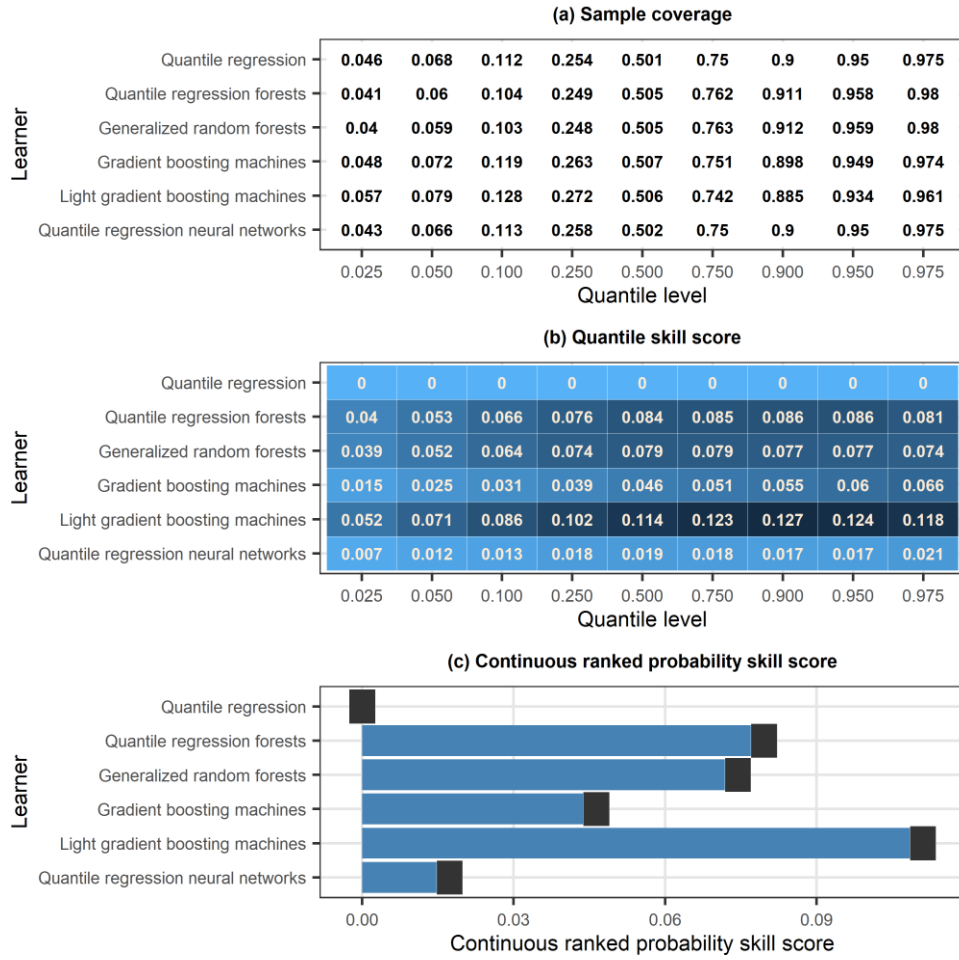


Figure 3. Statistics for facilitating the evaluation and comparison of the learners based on the entire dataset. Specifically: (a) Sample coverage of the learners at the various quantile levels; (b) quantile skill score of the learners at the various quantile levels; and (c) continuous ranked probability skill score of the learners. For interpreting (a): The closest the sample coverage to the quantile level, the more reliable the quantile predictions on average. For interpreting (b): The larger the quantile skill score (and the darker the colour on the respective heatmap), the better the quantile predictions on average compared to the quantile predictions of the benchmark learner (i.e., quantile regression). For interpreting (c): The larger the continuous ranked probability skill score, the better the probabilistic predictions on average compared to the probabilistic predictions of the benchmark learner (i.e., quantile regression).

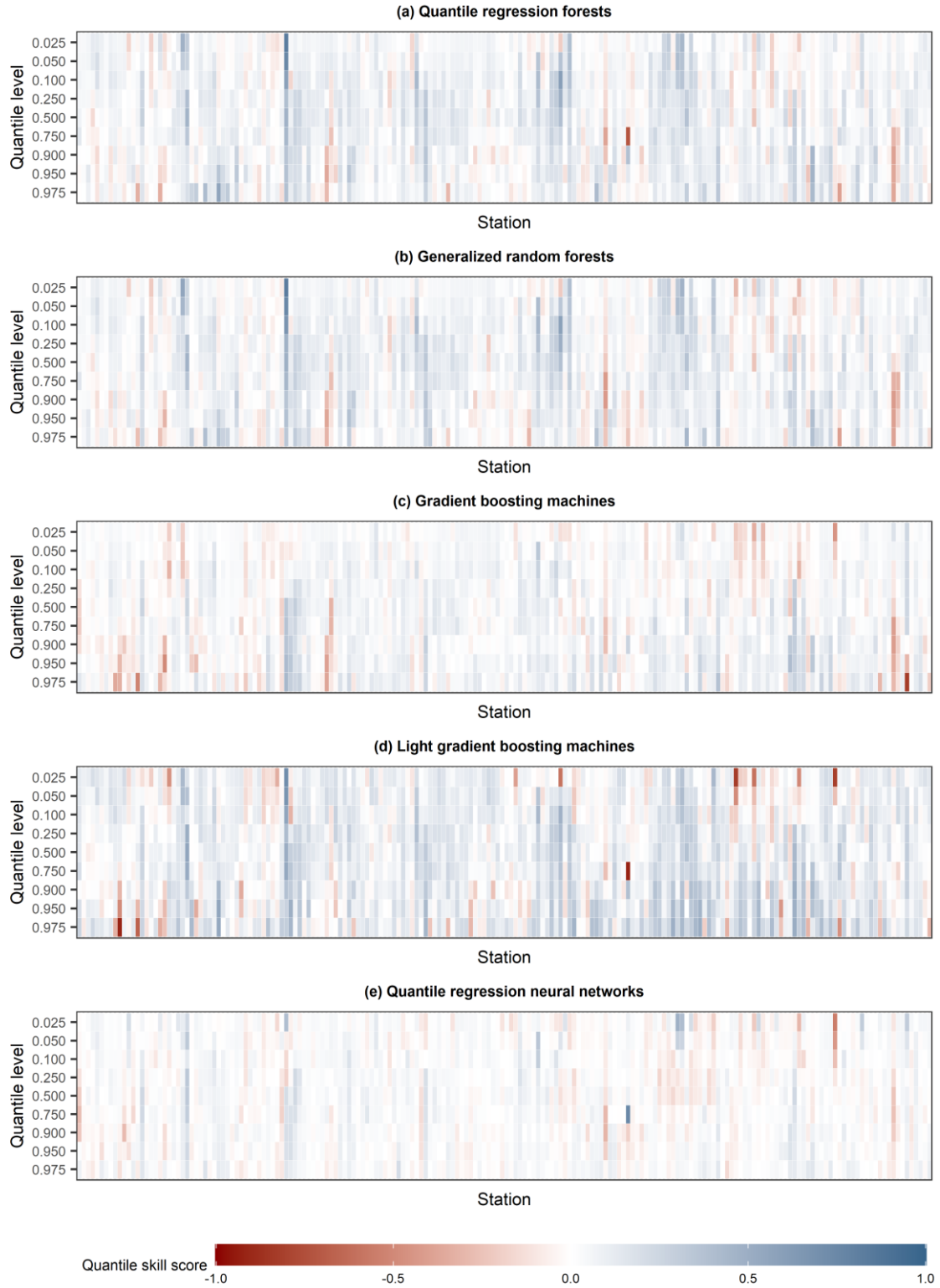


Figure 4. Quantile skill score of (a) quantile regression forests, (b) generalized random forests, (c) gradient boosting machines, (d) light gradient boosting machines and (e) quantile regression neural networks at the various quantile levels for 200 arbitrary stations. The larger the quantile skill score (and the darker blue the colour on the heatmaps), the better the quantile predictions on average compared to the quantile predictions of the benchmark learner (i.e., quantile regression).

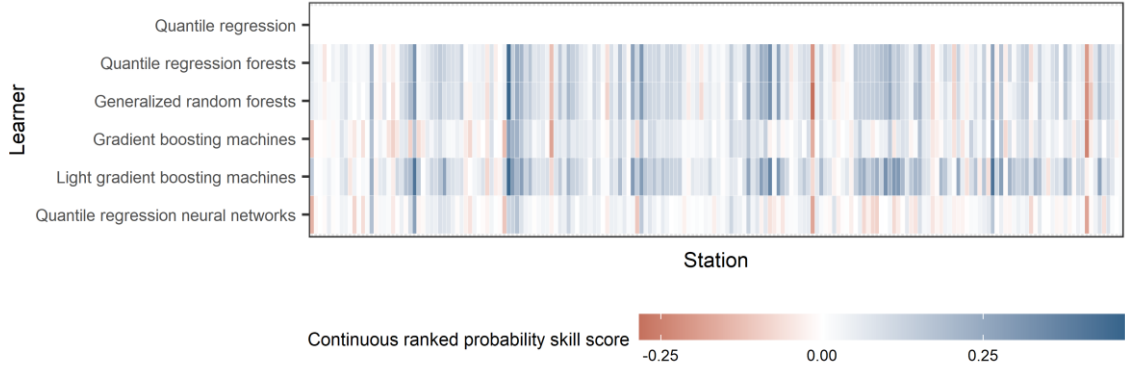


Figure 5. Continuous ranked probability skill score of the learners for the same stations as in [Figure 4](#). The larger the continuous ranked probability skill score (and the darker blue the colour on the heatmap), the better the probabilistic predictions on average compared to the probabilistic predictions of the benchmark learner (i.e., quantile regression).

4.2 Predictor variable importance comparison

[Figure 6](#) facilitates a comparison of the predictors with respect to their importance for the various quantile levels in the task of estimating predictive uncertainty while blending precipitation data from satellites and ground-based gauges. The respective results are largely homogenous across quantile levels, with IMERG value 1 and 2 being identified as the most and the second most important predictors by the LightGBM algorithm. The remaining IMERG values and the PERSIANN values are most often ranked before the distances with few exceptions, and the elevation of the station is also ranked third or fourth for the quantile levels {0.250, 0.500, 0.750, 0.900, 0.950, 0.975} and eighth or ninth for the remaining quantile levels.

5. Discussion

The large-scale benchmark experiment of this work suggests that LightGBM is the best-performing learner for uncertainty quantification in blending precipitation data from satellites and ground-based gauges at the monthly temporal scale, leaving QRF, GRF, GBM, QRNN and QR behind. In our view, this is an important finding, given also that LightGBM have at least similar or considerably lower computation requirements than other sophisticated learners for uncertainty quantification and have been proven useful when the interest is on extreme events (Tyrallis et al. [2023a](#)).

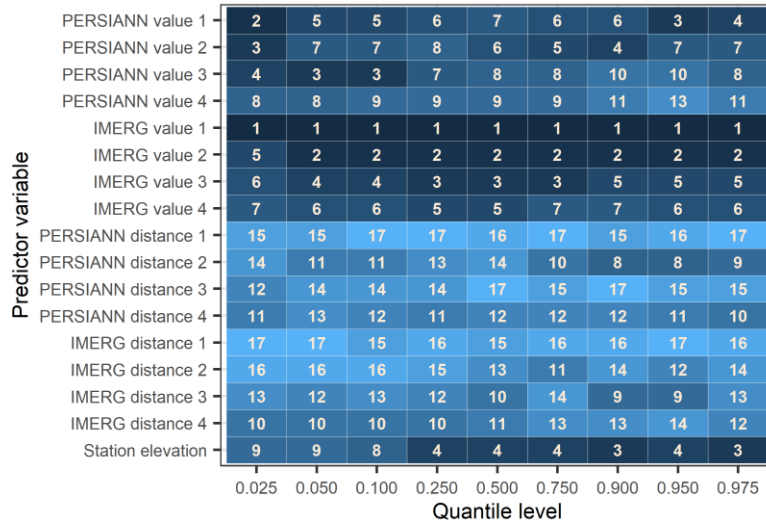


Figure 6. Ranking of the predictors from the most (1st) to the least (17th) important ones at the various quantile levels based on the gain statistic computed through light gradient boosting machines by exploiting the entire dataset. The darker the colour on the heatmap, the more important the predictor variable.

Furthermore, the feature importance tests showed that satellite precipitation variables are more important predictors than the elevation at a point of interest, which is a more important predictor than distances between a point of interest and satellite grid points. This outcome agrees with results by Papacharalampous et al. (2023c), a study on satellite precipitation product correction that did not involve uncertainty quantification.

Future research could focus on potential benefits that could stem from the application of the ensemble learning concept (Wang et al. 2022) for dealing with the general task of interest. Such investigations could focus both on simple ways to combine algorithms (e.g., the one in Petropoulos and Svetunkov 2020) and on advanced stacked generalization procedures (e.g., those in Wolpert 1992), and could use the learners implemented and compared in this work as base learners in the ensemble learning. They could also benefit from the comparative framework of this work.

Another idea for future research is to extend the comparison to other families of machine learning algorithms for predictive uncertainty quantification. Summaries of such families and their known properties are available in the reviews by Papacharalampous and Tyralis (2022) and Tyralis and Papacharalampous (2023). Lastly, potential benefits from incorporating time series features, such as those computed in Kang et al. (2017), into the predictive uncertainty quantification frameworks in the field of satellite precipitation product correction could be investigated.

6. Summary and conclusions

This is the first general study on the use of machine learning for the important, yet rarely performed, task of estimating predictive uncertainty in merging precipitation data from satellites and ground-based gauges. The concept of quantile regression was extensively investigated for the first time for fulfilling this task. To provide useful guidance on how this concept can be exploited, a large-scale comparison was conducted between quantile regression (QR), quantile regression forests (QRF), generalized random forests (GRF), gradient boosting machines (GBM), light gradient boosting machines (LightGBM) and quantile regression neural networks (QRNN). The comparison took place at the monthly temporal scale using 15-year-long data that span across the contiguous United States.

Such a large-scale benchmark study was indeed necessary, as the relative performance of the various learners can vary substantially from problem to problem and can only be assessed by taking advantage of large datasets. In the context of interest, LightGBM was identified as the best-performing learner for predictive uncertainty estimation based on the quantile and continuous ranked probability skill scores. The order from the best to the worst of the remaining algorithms is the following: QRF, GRF, GBM, QRNN and QR.

Lastly, the concept of feature importance was exploited through LightGBM to rank the predictors from the most to the least important ones for predictive uncertainty estimation in blending monthly precipitation data from satellites and ground-based gauges, thereby ensuring an adequate degree of interpretability.

Conflicts of interest: There is no conflict of interest.

Funding: This work was conducted in the context of the research project BETTER RAIN (BEnefitTING from machine LEarning algoRithms and concepts for correcting satellite RAINfall products). This research project was supported by the Hellenic Foundation for Research and Innovation (H.F.R.I.) under the “3rd Call for H.F.R.I. Research Projects to support Post-Doctoral Researchers” (Project Number: 7368).

Acknowledgements: Currently not applicable.

Data availability statement: No new data were created or analysed in this study. The datasets used are cited in the manuscript.

Ethical statement: Not applicable.

Appendix A Statistical software

The R programming language (R Core Team 2023) was used for processing the data, for implementing the learners, and for reporting and visualizing the results. The following R packages were used: `caret` (Kuhn 2023), `data.table` (Dowle and Srinivasan 2023), `devtools` (Wickham et al. 2022), `elevatr` (Hollister 2023), `gbm` (Greenwell et al. 2022), `grf` (Tibshirani and Athey 2023), `knitr` (Xie 2014, 2015, 2023), `lightgbm` (Shi et al. 2023), `ncdf4` (Pierce 2023), `qrrn` (Cannon 2011, 2018, 2023), `quantreg` (Koenker 2023), `rgdal` (Bivand et al. 2023), `rmarkdown` (Allaire et al. 2023, Xie et al. 2018, 2020), `scoringfunctions` (Tyrallis and Papacharalampous 2022, 2023), `sf` (Pebesma 2018, 2023), `spdep` (Bivand 2023, Bivand and Wong 2018, Bivand et al. 2013) and `tidyverse` (Wickham et al. 2019, Wickham 2023).

References

- [1] Abdollahipour A, Ahmadi H, Aminnejad B (2022) A review of downscaling methods of satellite-based precipitation estimates. *Earth Science Informatics* 15(1):1–20. <https://doi.org/10.1007/s12145-021-00669-4>.
- [2] Allaire JJ, Xie Y, McPherson J, Luraschi J, Ushey K, Atkins A, Wickham H, Cheng J, Chang W, Iannone R (2023) `rmarkdown`: Dynamic Documents for R. R package version 2.21. <https://CRAN.R-project.org/package=rmarkdown>.
- [3] Athey S, Tibshirani J, Wager S (2019) Generalized random forests. *Annals of Statistics* 47(2):1148–1178. <https://doi.org/10.1214/18-AOS1709>.
- [4] Baez-Villanueva OM, Zambrano-Bigiarini M, Beck HE, McNamara I, Ribbe L, Nauditt A, Birkel C, Verbist K, Giraldo-Osorio JD, Xuan Thinh N (2020) RF-MEP: A novel random forest method for merging gridded precipitation products and ground-based measurements. *Remote Sensing of Environment* 239:111606. <https://doi.org/10.1016/j.rse.2019.111606>.
- [5] Bhuiyan MAE, Nikolopoulos EI, Anagnostou EN, Quintana-Seguí P, Barella-Ortiz A (2018) A nonparametric statistical technique for combining global precipitation datasets: Development and hydrological evaluation over the Iberian Peninsula. *Hydrology and Earth System Sciences* 22(2):1371–1389. <https://doi.org/10.5194/hess-22-1371-2018>.
- [6] Bivand RS (2023) `spdep`: Spatial Dependence: Weighting Schemes, Statistics. R package version 1.2-8. <https://CRAN.R-project.org/package=spdep>.
- [7] Bivand RS, Wong DWS (2018) Comparing implementations of global and local indicators of spatial association. *TEST* 27(3):716–748. <https://doi.org/10.1007/s11749-018-0599-x>.
- [8] Bivand RS, Pebesma E, Gómez-Rubio V (2013) *Applied Spatial Data Analysis with R*. Second Edition. Springer New York, NY. <https://doi.org/10.1007/978-1-4614-7618-4>.
- [9] Bivand RS, Keitt T, Rowlingson B (2023) `rgdal`: Bindings for the ‘Geospatial’ Data Abstraction Library. R package version 1.6-6. <https://CRAN.R-project.org/package=rgdal>.

- [10] Boulesteix AL, Binder H, Abrahamowicz M, Sauerbrei W (2018) Simulation Panel of the STRATOS Initiative. On the necessity and design of studies comparing statistical methods. *Biometrical Journal* 60(1):216–218. <https://doi.org/10.1002/bimj.201700129>.
- [11] Breiman L (1996) Bagging predictors. *Machine Learning* 24(2):123–140. <https://doi.org/10.1007/BF00058655>.
- [12] Breiman L (2001) Random forests. *Machine Learning* 45(1):5–32. <https://doi.org/10.1023/A:1010933404324>.
- [13] Breiman L, Friedman J, Stone CJ, Olshen RA (1984) *Classification and Regression Trees*. First Edition. Chapman & Hall/CRC: Boca Raton, FL, USA.
- [14] Bröcker J (2012) Evaluating raw ensembles with the continuous ranked probability score. *Quarterly Journal of the Royal Meteorological Society* 138(667):1611–1617. <https://doi.org/10.1002/qj.1891>.
- [15] Cannon AJ (2011) Quantile regression neural networks: Implementation in R and application to precipitation downscaling. *Computers and Geosciences* 37(9):1277–1284. <https://doi.org/10.1016/j.cageo.2010.07.005>.
- [16] Cannon AJ (2018) Non-crossing nonlinear regression quantiles by monotone composite quantile regression neural network, with application to rainfall extremes. *Stochastic Environmental Research and Risk Assessment* 32(11):3207–3225. <https://doi.org/10.1007/s00477-018-1573-6>.
- [17] Cannon AJ (2023) qrn: Quantile Regression Neural Network. R package version 2.1. <https://CRAN.R-project.org/package=qrn>.
- [18] Chen H, Chandrasekar V, Cifelli R, Xie P (2020) A machine learning system for precipitation estimation using satellite and ground radar network observations. *IEEE Transactions on Geoscience and Remote Sensing* 58(2):982–994. <https://doi.org/10.1109/TGRS.2019.2942280>.
- [19] Dowle M, Srinivasan A (2023) data.table: Extension of 'data.frame'. R package version 1.14.8. <https://CRAN.R-project.org/package=data.table>.
- [20] Cui W, Wan C, Song Y (2022) Ensemble deep learning-based non-crossing quantile regression for nonparametric probabilistic forecasting of wind power generation. *IEEE Transactions on Power Systems*. <https://doi.org/10.1109/TPWRS.2022.3202236>.
- [21] Efron B, Hastie T (2016) *Computer Age Statistical Inference*. Cambridge University Press, New York. <https://doi.org/10.1017/CBO9781316576533>.
- [22] Epstein E (1969) A scoring system for probability forecasts of ranked categories. *Journal of Applied Meteorology and Climatology* 8(6):985–987. [https://doi.org/10.1175/1520-0450\(1969\)008<0985:ASSFPF>2.0.CO;2](https://doi.org/10.1175/1520-0450(1969)008<0985:ASSFPF>2.0.CO;2).
- [23] Fernandez-Palomino CA, Hattermann FF, Krysanova V, Lobanova A, Vega-Jácome F, Lavado W, Santini W, Aybar C, Bronstert A (2022) A novel high-resolution gridded precipitation dataset for Peruvian and Ecuadorian watersheds: Development and hydrological evaluation. *Journal of Hydrometeorology* 23(3):309–336. <https://doi.org/10.1175/JHM-D-20-0285.1>.
- [24] Friedman JH (2001) Greedy function approximation: A gradient boosting machine. *The Annals of Statistics* 29(5):1189–1232. <https://doi.org/10.1214/aos/1013203451>.
- [25] Glawion L, Polz J, Kunstmann HG, Fersch B, Chwala C (2023) spateGAN: Spatio-temporal downscaling of rainfall fields using a cGAN approach. <https://doi.org/10.22541/essoar.167690003.33629126/v1>.

- [26] Gneiting T (2011) Making and evaluating point forecasts. *Journal of the American Statistical Association* 106(494):746–762. <https://doi.org/10.1198/jasa.2011.r10138>.
- [27] Gneiting T, Raftery AE (2007) Strictly proper scoring rules, prediction, and estimation. *Journal of the American Statistical Association* 102(477):359–378. <https://doi.org/10.1198/016214506000001437>.
- [28] Greenwell B, Boehmke B, Cunningham J, et al. (2022) gbm: Generalized Boosted Regression Models. R package version 2.1.8.1. <https://CRAN.R-project.org/package=gbm>.
- [29] Hastie T, Tibshirani R, Friedman J (2009) *The Elements of Statistical Learning*. Springer, New York. <https://doi.org/10.1007/978-0-387-84858-7>.
- [30] He Y, Qin Y, Wang S, Wang X, Wang C (2019) Electricity consumption probability density forecasting method based on LASSO-Quantile Regression Neural Network. *Applied Energy* 233–234:565–575. <https://doi.org/10.1016/j.apenergy.2018.10.061>.
- [31] Hollister JW (2023) elevatr: Access Elevation Data from Various APIs. R package version 0.99.0. <https://CRAN.R-project.org/package=elevatr>.
- [32] Hsu K-L, Gao X, Sorooshian S, Gupta HV (1997) Precipitation estimation from remotely sensed information using artificial neural networks. *Journal of Applied Meteorology* 36(9):1176–1190. [https://doi.org/10.1175/1520-0450\(1997\)036<1176:PEFRSI>2.0.CO;2](https://doi.org/10.1175/1520-0450(1997)036<1176:PEFRSI>2.0.CO;2).
- [33] Hu Q, Li Z, Wang L, Huang Y, Wang Y, Li L (2019) Rainfall spatial estimations: A review from spatial interpolation to multi-source data merging. *Water* 11(3):579. <https://doi.org/10.3390/w11030579>.
- [34] Huffman GJ, Stocker EF, Bolvin DT, Nelkin EJ, Tan J (2019) GPM IMERG Late Precipitation L3 1 day 0.1 degree x 0.1 degree V06, Edited by Andrey Savtchenko, Greenbelt, MD, Goddard Earth Sciences Data and Information Services Center (GES DISC), Accessed: [2022-10-12], <https://doi.org/10.5067/GPM/IMERGDL/DAY/06>.
- [35] James G, Witten D, Hastie T, Tibshirani R (2013) *An Introduction to Statistical Learning*. Springer, New York. <https://doi.org/10.1007/978-1-4614-7138-7>.
- [36] Kang Y, Hyndman RJ, Smith-Miles K (2017) Visualising forecasting algorithm performance using time series instance spaces. *International Journal of Forecasting* 33(2):345–358. <https://doi.org/10.1016/j.ijforecast.2016.09.004>.
- [37] Kasraei B, Heung B, Saurette DD, Schmidt MG, Bulmer CE, Bethel W (2021) Quantile regression as a generic approach for estimating uncertainty of digital soil maps produced from machine-learning. *Environmental Modelling and Software* 144:105139. <https://doi.org/10.1016/j.envsoft.2021.105139>.
- [38] Ke G, Meng Q, Finley T, Wang T, Chen W, Ma W, Ye Q, Liu TY (2017) Lightgbm: A highly efficient gradient boosting decision tree. *Advances in Neural Information Processing Systems* 30:3146–3154.
- [39] Koenker RW (2005) *Quantile regression*. Cambridge University Press, Cambridge, UK.
- [40] Koenker RW (2023) quantreg: Quantile Regression. R package version 5.97. <https://CRAN.R-project.org/package=quantreg>.
- [41] Koenker RW, Bassett Jr G (1978). Regression quantiles. *Econometrica* 46(1):33–50. <https://doi.org/10.2307/1913643>.
- [42] Kuhn M (2023) caret: Classification and Regression Training. R package version 6.0-94. <https://CRAN.R-project.org/package=caret>.

- [43] Matheson JE, Winkler RL (1976) Scoring rules for continuous probability distributions. *Management Science* 22(10):1087–1096. <https://doi.org/10.1287/mnsc.22.10.1087>.
- [44] Mayr A, Binder H, Gefeller O, Schmid M (2014) The evolution of boosting algorithms: From machine learning to statistical modelling. *Methods of Information in Medicine* 53(6):419–427. <https://doi.org/10.3414/ME13-01-0122>.
- [45] Meinshausen N, Ridgeway G (2006) Quantile regression forests. *Journal of Machine Learning Research* 7:983–999.
- [46] Nguyen P, Ombadi M, Sorooshian S, Hsu K, AghaKouchak A, Braithwaite D, Ashouri H, Rose Thorstensen A (2018) The PERSIANN family of global satellite precipitation data: A review and evaluation of products. *Hydrology and Earth System Sciences* 22(11):5801–5816. <https://doi.org/10.5194/hess-22-5801-2018>.
- [47] Nguyen P, Shearer EJ, Tran H, Ombadi M, Hayatbini N, Palacios T, Huynh P, Braithwaite D, Updegraff G, Hsu K, Kuligowski B, Logan WS, Sorooshian S (2019) The CHRS data portal, an easily accessible public repository for PERSIANN global satellite precipitation data. *Scientific Data* 6:180296. <https://doi.org/10.1038/sdata.2018.296>.
- [48] Nguyen GV, Le X-H, Van LN, Jung S, Yeon M, Lee G (2021) Application of random forest algorithm for merging multiple satellite precipitation products across South Korea. *Remote Sensing* 13(20):4033. <https://doi.org/10.3390/rs13204033>.
- [49] Papacharalampous G, Tyralis H (2022) A review of machine learning concepts and methods for addressing challenges in probabilistic hydrological post-processing and forecasting. *Frontiers in Water* 4:961954. <https://doi.org/10.3389/frwa.2022.961954>.
- [50] Papacharalampous GA, Koutsoyiannis D, Montanari A (2020) Quantification of predictive uncertainty in hydrological modelling by harnessing the wisdom of the crowd: Methodology development and investigation using toy models. *Advances in Water Resources* 136:103471. <https://doi.org/10.1016/j.advwatres.2019.103471>.
- [51] Papacharalampous GA, Tyralis H, Doulamis A, Doulamis N (2023a) Comparison of machine learning algorithms for merging gridded satellite and earth-observed precipitation data. *Water* 15(4):634. <https://doi.org/10.3390/w15040634>.
- [52] Papacharalampous GA, Tyralis H, Doulamis A, Doulamis N (2023b) Comparison of tree-based ensemble algorithms for merging satellite and earth-observed precipitation data at the daily time scale. *Hydrology* 10(2):50. <https://doi.org/10.3390/hydrology10020050>.
- [53] Papacharalampous GA, Tyralis H, Doulamis N, Doulamis A (2023c) Ensemble learning for blending gridded satellite and gauge-measured precipitation data. *Remote Sensing* 15(20):4912. <https://doi.org/10.3390/rs15204912>.
- [54] Pebesma E (2018) Simple features for R: Standardized support for spatial vector data. *The R Journal* 10(1):439–446. <https://doi.org/10.32614/RJ-2018-009>.
- [55] Pebesma E (2023) sf: Simple Features for R. R package version 1.0-13. <https://CRAN.R-project.org/package=sf>.

- [56] Peterson TC, Vose RS (1997) An overview of the Global Historical Climatology Network temperature database. *Bulletin of the American Meteorological Society* 78(12):2837–2849. [https://doi.org/10.1175/1520-0477\(1997\)078<2837:A00TGH>2.0.CO;2](https://doi.org/10.1175/1520-0477(1997)078<2837:A00TGH>2.0.CO;2).
- [57] Petropoulos F, Svetunkov I (2020) A simple combination of univariate models. *International Journal of Forecasting* 36(1):110–115. <https://doi.org/10.1016/j.ijforecast.2019.01.006>.
- [58] Pierce D (2023) ncd4: Interface to Unidata netCDF (Version 4 or Earlier) Format Data Files. R package version 1.21. <https://CRAN.R-project.org/package=ncdf4>.
- [59] R Core Team (2023) R: A language and environment for statistical computing. R Foundation for Statistical Computing, Vienna, Austria. <https://www.r-project.org>.
- [60] Rodrigues F, Pereira FC (2020) Beyond expectation: Deep joint mean and quantile regression for spatiotemporal problems. *IEEE Transactions on Neural Networks and Learning Systems* 31(12):5377–5389. <https://doi.org/10.1109/TNNLS.2020.2966745>.
- [61] Sagi O, Rokach L (2018) Ensemble learning: A survey. *Wiley Interdisciplinary Reviews: Data Mining and Knowledge Discovery* 8(4):e1249. <https://doi.org/10.1002/widm.1249>.
- [62] Sesia M, Candès EJ (2020) A comparison of some conformal quantile regression methods. *Stat* 9(1):e261. <https://doi.org/10.1002/sta4.261>.
- [63] Shi Y, Ke G, Soukhavong D, Lamb J, Meng Q, Finley T, Wang T, Chen W, Ma W, Ye Q, Liu T-Y, Titov N. (2023) lightgbm: Light Gradient Boosting Machine. R package version 3.3.5. <https://CRAN.R-project.org/package=lightgbm>.
- [64] Tareghian R, Rasmussen PF (2013) Statistical downscaling of precipitation using quantile regression. *Journal of Hydrology* 487:122–135. <https://doi.org/10.1016/j.jhydrol.2013.02.029>.
- [65] Taylor JW (2000) A quantile regression neural network approach to estimating the conditional density of multiperiod returns. *Journal of Forecasting* 19(4):299–311. [https://doi.org/10.1002/1099-131X\(200007\)19:4<299::AID-FOR775>3.0.CO;2-V](https://doi.org/10.1002/1099-131X(200007)19:4<299::AID-FOR775>3.0.CO;2-V).
- [66] Tibshirani J, Athey S (2023) grf: Generalized Random Forests. R package version 2.3.1. <https://cran.r-project.org/package=grf>.
- [67] Tyralis H, Papacharalampous G (2021a) Boosting algorithms in energy research: A systematic review. *Neural Computing and Applications* 33(21):14101–14117. <https://doi.org/10.1007/s00521-021-05995-8>.
- [68] Tyralis H, Papacharalampous GA (2021b) Quantile-based hydrological modelling. *Water* 13(23):3420. <https://doi.org/10.3390/w13233420>.
- [69] Tyralis H, Papacharalampous G (2022) A review of probabilistic forecasting and prediction with machine learning. <https://arxiv.org/abs/2209.08307>.
- [70] Tyralis H, Papacharalampous G (2023) scoringfunctions: A Collection of Scoring Functions for Assessing Point Forecasts. R package version 0.0.6. <https://CRAN.R-project.org/package=scoringfunctions>.
- [71] Tyralis H, Papacharalampous GA, Doulamis N, Doulamis A (2023a) Merging satellite and gauge-measured precipitation using LightGBM with an emphasis on extreme quantiles. *IEEE Journal of Selected Topics in Applied Earth Observations and Remote Sensing* 16:6969–6979. <https://doi.org/10.1109/JSTARS.2023.3297013>.

- [72] Tyralis H, Papacharalampous GA, Khatami S (2023b) Expectile-based hydrological modelling for uncertainty estimation: Life after mean. *Journal of Hydrology* 617(Part B):128986. <https://doi.org/10.1016/j.jhydrol.2022.128986>.
- [73] Waldmann E (2018) Quantile regression: A short story on how and why. *Statistical Modelling* 18(3–4):203–218. <https://doi.org/10.1177/1471082X18759142>.
- [74] Wang X, Hyndman RJ, Li F, Kang Y (2022) Forecast combinations: An over 50-year review. *International Journal of Forecasting*. <https://doi.org/10.1016/j.ijforecast.2022.11.005>.
- [75] Weerts AH, Winsemius HC, Verkade JS (2011) Estimation of predictive hydrological uncertainty using quantile regression: Examples from the National Flood Forecasting System (England and Wales). *Hydrology and Earth System Sciences* 15(1):255–265. <https://doi.org/10.5194/hess-15-255-2011>.
- [76] Wickham H (2023) tidyverse: Easily Install and Load the 'Tidyverse'. R package version 2.0.0. <https://CRAN.R-project.org/package=tidyverse>.
- [77] Wickham H, Averick M, Bryan J, Chang W, McGowan LD, François R, Golemund G, Hayes A, Henry L, Hester J, Kuhn M, Pedersen TL, Miller E, Bache SM, Müller K, Ooms J, Robinson D, Paige Seidel DP, Spinu V, Takahashi K, Vaughan D, Wilke C, Woo K, Yutani H (2019) Welcome to the tidyverse. *Journal of Open Source Software* 4(43):1686. <https://doi.org/10.21105/joss.01686>.
- [78] Wickham H, Hester J, Chang W, Bryan J (2022) devtools: Tools to Make Developing R Packages Easier. R package version 2.4.5. <https://CRAN.R-project.org/package=devtools>.
- [79] Wolpert DH (1992) Stacked generalization. *Neural Networks* 5(2):241–259. [https://doi.org/10.1016/S0893-6080\(05\)80023-1](https://doi.org/10.1016/S0893-6080(05)80023-1).
- [80] Xie Y (2014) knitr: A Comprehensive Tool for Reproducible Research in R. In: Stodden V, Leisch F, Peng RD (Eds) *Implementing Reproducible Computational Research*. Chapman and Hall/CRC.
- [81] Xie Y (2015) *Dynamic Documents with R and knitr*, 2nd edition. Chapman and Hall/CRC.
- [82] Xie Y (2023) knitr: A General-Purpose Package for Dynamic Report Generation in R. R package version 1.44. <https://CRAN.R-project.org/package=knitr>.
- [83] Xie Y, Allaire JJ, Golemund G (2018) *R Markdown: The Definitive Guide*. Chapman and Hall/CRC. ISBN 9781138359338. <https://bookdown.org/yihui/rmarkdown>.
- [84] Xie Y, Dervieux C, Riederer E (2020) *R Markdown Cookbook*. Chapman and Hall/CRC. ISBN 9780367563837. <https://bookdown.org/yihui/rmarkdown-cookbook>.
- [85] Xiong L, Li S, Tang G, Strobl J (2022) Geomorphometry and terrain analysis: Data, methods, platforms and applications. *Earth-Science Reviews* 233:104191. <https://doi.org/10.1016/j.earscirev.2022.104191>.
- [86] Zhang W, Quan H, Srinivasan D (2018) Parallel and reliable probabilistic load forecasting via quantile regression forest and quantile determination. *Energy* 160:810–819. <https://doi.org/10.1016/j.energy.2018.07.019>.
- [87] Zhang Y, Ye A, Nguyen P, Analui B, Sorooshian S, Hsu K (2022) QRF4P-NRT: Probabilistic post-processing of near-real-time satellite precipitation estimates using quantile regression forests. *Water Resources Research* 58(5):e2022WR032117. <https://doi.org/10.1029/2022WR032117>.